Supplemental Information

In-drop thermal cycling of microcrystal assembly for senescence control (MASC) with minimal variation in efficacy

Ryan C. Miller[a], Jonghwi Lee[b], Young Jun Kim[c], Hee-Sun Han[d,e,*], Hyunjoon Kong[a,e,*]

[a] Department of Chemical and Biomolecular Engineering, University of Illinois at Urbana-Champaign, Urbana, IL 61801, USA

[b] Department of Chemical Engineering and Materials Science, Chung-Ang University, Seoul 06974, Korea

[c] Environmental Safety Group, Korea Institute of Science and Technology-Europe, Saarbrucken 66123, Germany

[d] Department of Chemistry, University of Illinois at Urbana-Champaign, Urbana, IL 61801, USA

[e] Institute for Genomic Biology, University of Illinois at Urbana-Champaign, Urbana, IL 61801, USA

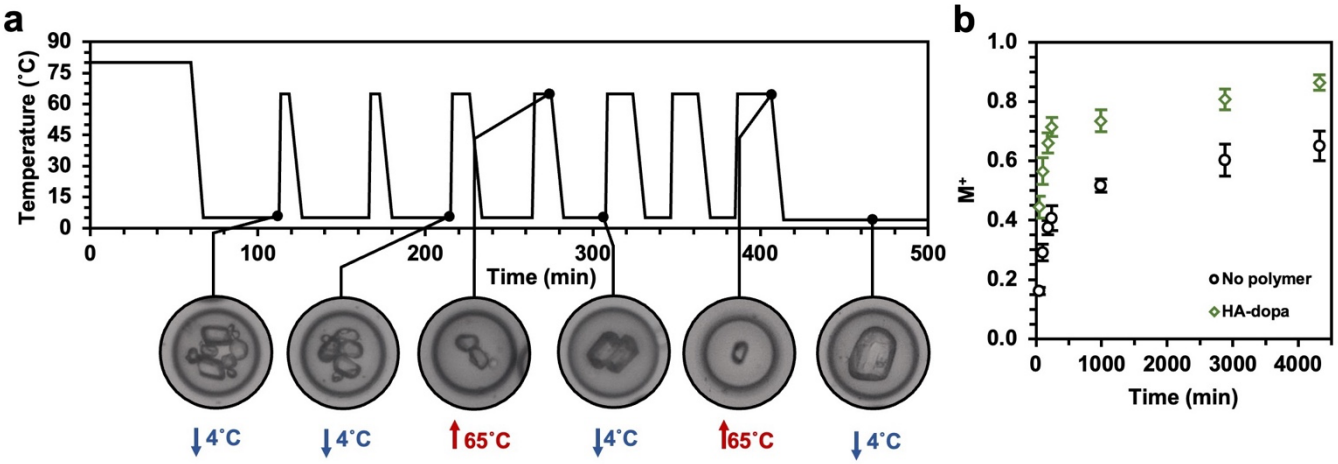

Figure S1: Thermal cycle conditions and effects of HA-dopa-induced nucleation in drops. (a) Temperature profiles for thermocycling NAC solution drops. Optical images of representative drops with crystals at different stages of thermocycling. **(b)** Fraction of drops containing a minimum of one crystal (M^+) over 75 hours for drops containing no polymer drops containing or drops containing 2.5wt% HA-dopa. Error bars represent 1 standard deviation of the mean. 250 drops were characterized for each condition.

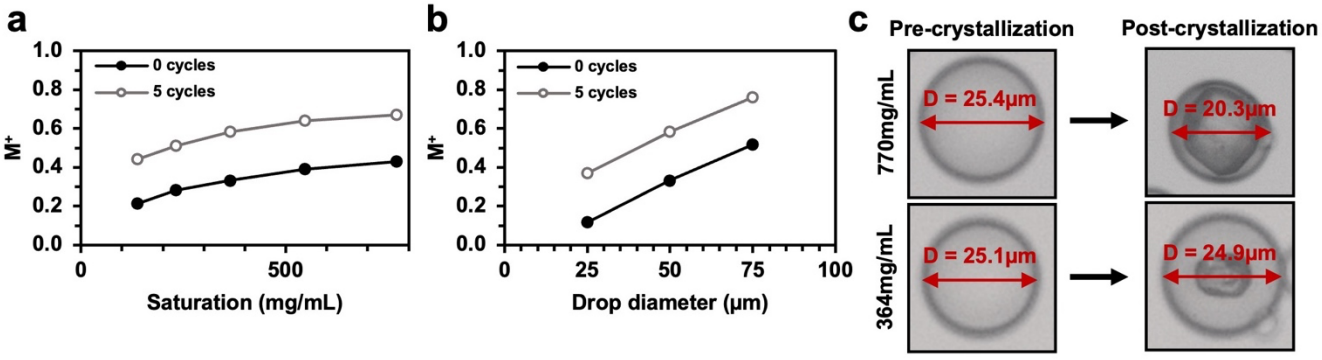

Figure S2: Nucleation efficiency and effect of thermocycling, starting saturation, and drop diameter. (a) Fraction of drops containing at least 1 crystal (M^+) with starting NAC concentrations ranging from 138-770mg/mL. A minimum of 250 drops were characterized for both 0 thermocycles and 5 thermocycles. Drop diameter fixed at 50μm. **(b)** Fraction of drops containing at least 1 crystal from drop diameters ranging from 25-75μm. A minimum of 250 drops were characterized for both 0 thermocycles and 5 thermocycles. Starting NAC concentration was fixed at 364mg/mL. **(c)** Representative optical images depicting drop diameters pre- and post-crystallization for NAC solutions saturated at either 770mg/mL or 364mg/mL.

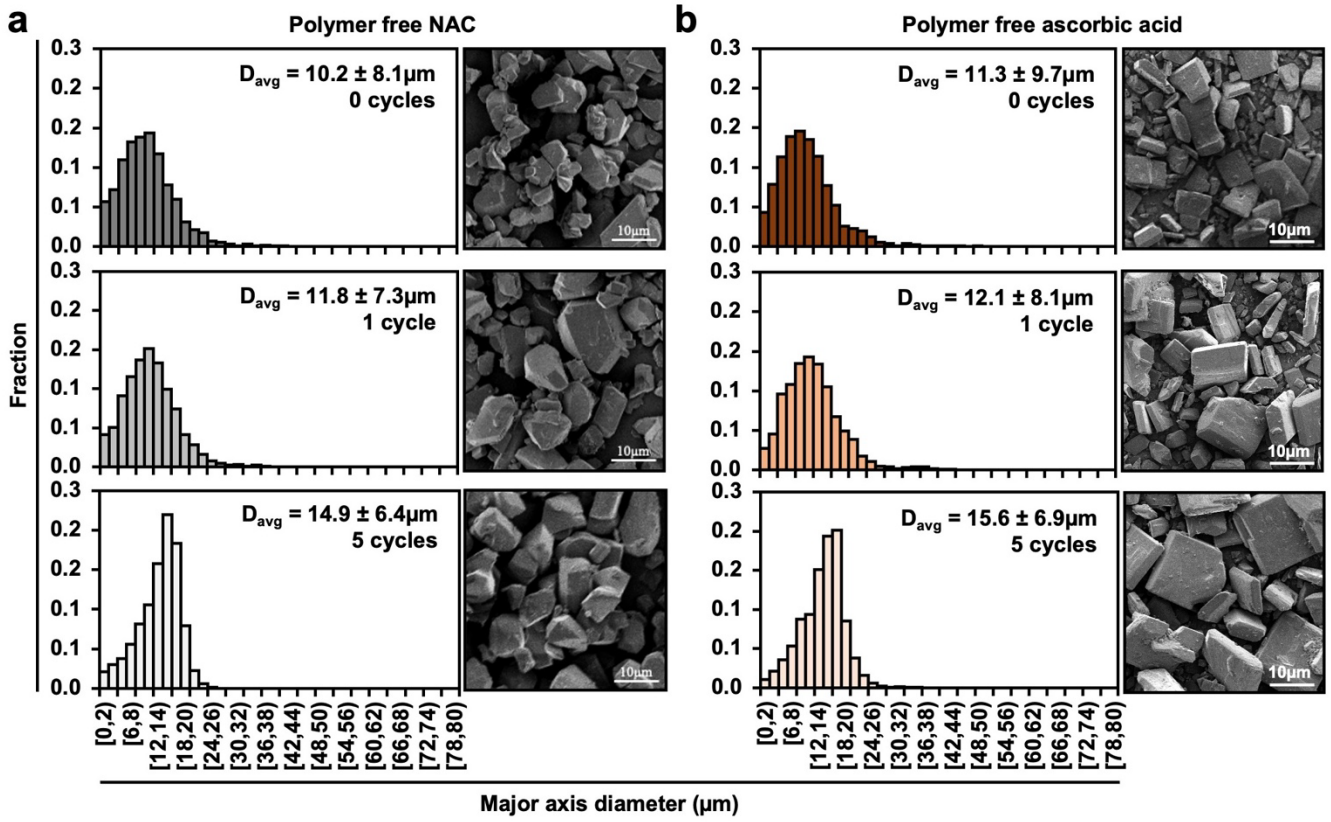

Figure S3: Thermocycling of antioxidant crystals. (a) Histograms and representative SEM images for NAC crystals fabricated and thermal cycled in 25µm-diameter drops. All crystals were prepared in the presence of no polymer and with a 364mg/mL starting NAC solution. **(c)** Histograms and representative SEM images for ascorbic acid crystals fabricated and thermal cycled in 25µm-diameter drops. All crystals were prepared with a 364mg/mL starting ascorbic acid solution. No HA-dopa was used. D_{avg} represents the average major axis diameter of the crystal population and one standard deviation. A minimum of 2,000 crystals were characterized for each population.

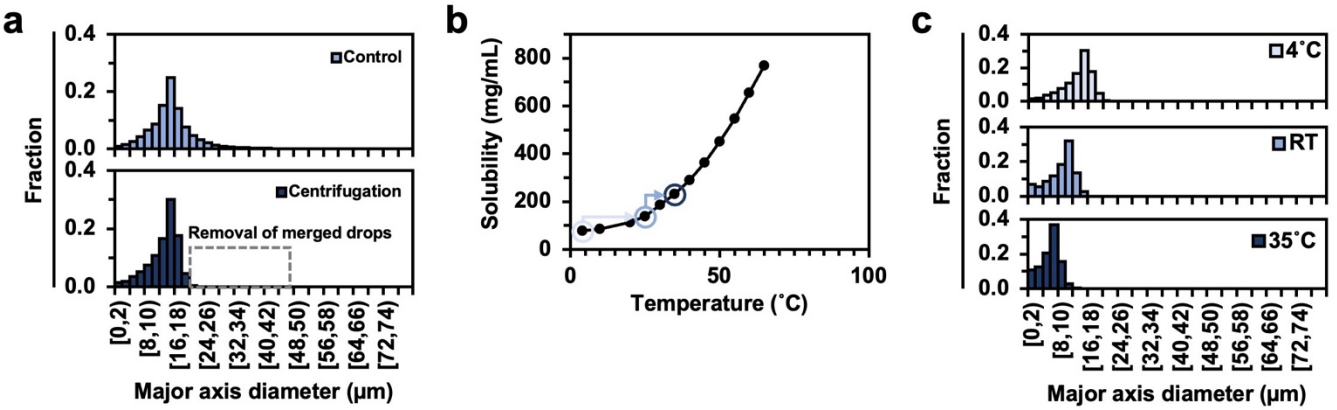

Figure S4: Post thermocycling processing of NAC crystals. (a) Histograms depicting the major axis diameter of NAC crystals obtained from single emulsion drops pre- and post-density gradient centrifugation to remove merged drops. The major axis diameter was determined from SEM images where a minimum of 2,000 crystals were characterized. **(b)** Solubility cure of NAC in DI water. Arrows depict post thermocycling temperature changes to increase the solubility of NAC. **(c)** Histograms depicting the major axis diameter of NAC crystals following heating steps from 4˚C to 25˚C and 35 ˚C. The major axis diameter was determined from SEM images where a minimum of 2,000 crystals were characterized.

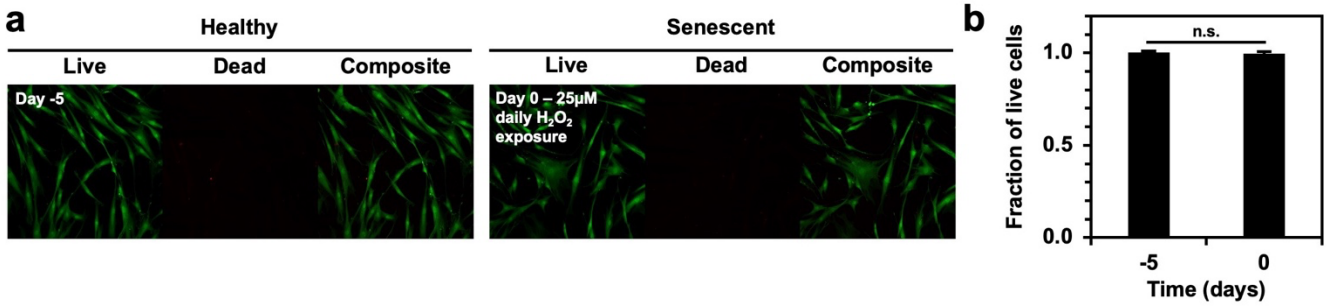

Figure S5: LIVE/DEAD assay. (a) Confocal images of healthy MSCs (never exposed to H_2O_2) and senescent MSCs. Green fluorescence depicts live cells and red fluorescence depicts dead cells. **(b)** Quantification of the fraction of live cells pre- and post-H2O2 exposure. *p < 0.05, **p < 0.01, ***p < 0.001 as determined by Wilcoxon rank sum test.

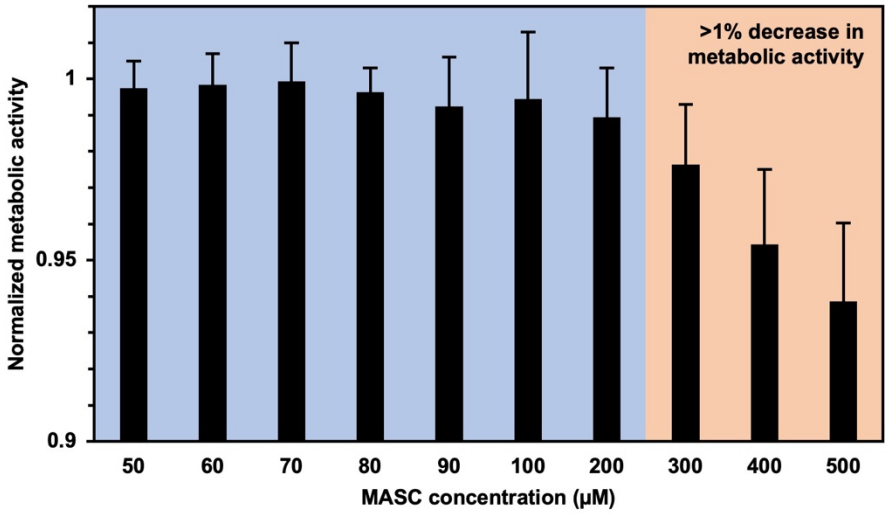

Figure S6: Metabolic activity of MSCs post MASC exposure. Metabolic activity of MSC population following MASC exposure every 2 days for 6 days. Metabolic activity normalized to metabolic activity of MSCs never exposed to MASC.

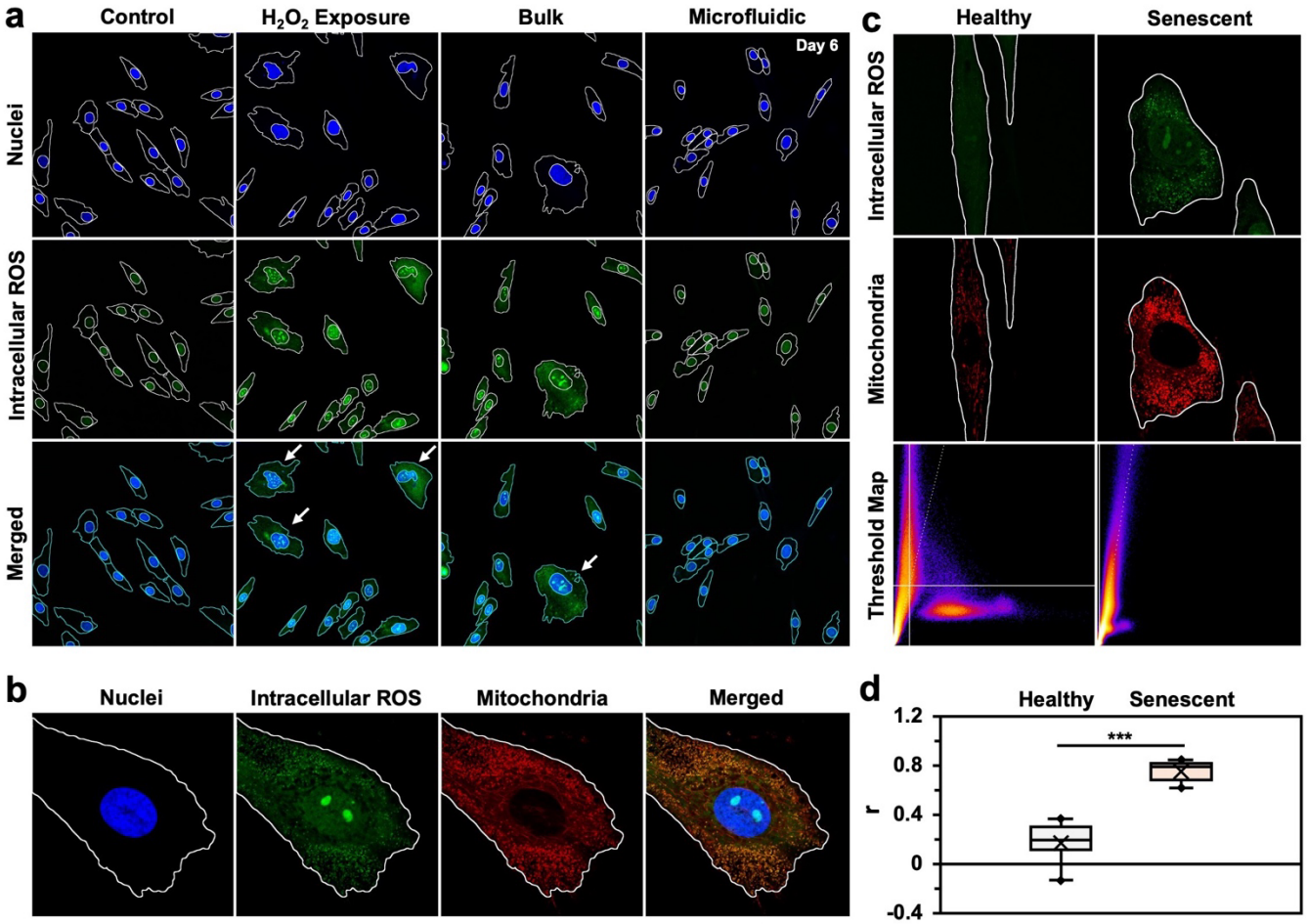

Figure S7: Antioxidizing NAC crystal modulation of intracellular ROS in MSCs in an acute senescent state and colocalization of intracellular ROS and the mitochondria. (a) Confocal images of intracellular oxidative stress in MSCs following no treatment, treatment with bulk-assembled crystals, and treatment with microfluidic-assembled NAC crystals for 6 days. The blue stain (DAPI) depicts the cell nuclei, and the green stain (CellROX Green) depicts intracellular ROS. White arrows point to MSCs with flattened senescent phenotype. **(b) 63x objective** confocal images of intracellular oxidative stress and mitochondria in MSCs following H_2O_2 exposure. The blue stain (DAPI) depicts the cell nuclei, the green stain (CellROX Green) depicts intracellular ROS, and the red stain (MitoTracker RED) depicts the mitochondria. **(c)** Representative confocal images of the intracellular ROS and mitochondria for a healthy cell and a senescent cell. The green stain (CellROX Green) depicts intracellular ROS, and the red stain (MitoTracker RED) depicts the mitochondria. The threshold maps depict the pixel intensities for the mitochondria (y-axis) and intracellular ROS (x-axis). **(b)** Box and whisker plots describing the Pearson's colocalization coefficient (r) for healthy and senescent cells. *$p < 0.05$, **$p < 0.01$, ***$p < 0.001$ as determined by Wilcoxon rank sum test.

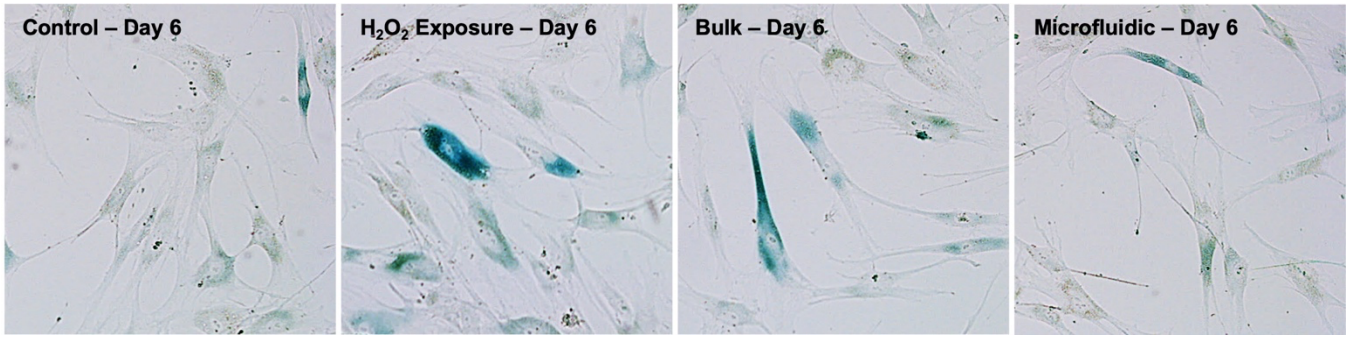

Figure S8: *β*-galactosidase histochemical stain. MSCs were exposed to 25μM H_2O_2 daily for 5 days and then either treated with NAC-free media, bulk-assembled NAC crystals, or microfluidic-assembled NAC crystals every two days for 6 days. The optical images depict staining at 6 days of NAC treatment, where blue stained cells depict β-galactosidase-positive MSCs.